

Relationships between regional coastal land cover distributions and elevation reveal data uncertainty in a sea-level rise impacts model

Erika E. Lentz¹, Nathaniel G. Plant², E. Robert Thieler¹

¹U.S. Geological Survey, Woods Hole Coastal and Marine Science Center, Woods Hole, MA 02543, USA

²U.S. Geological Survey, St. Petersburg Coastal and Marine Science Center, St. Petersburg, FL 33701, USA

Correspondence to: Erika E. Lentz (elentz@usgs.gov)

Abstract. Understanding land loss or resilience in response to sea-level rise (SLR) requires spatially extensive and continuous datasets to capture landscape variability. We investigate sensitivity and skill of a model that predicts dynamic response likelihood to SLR across the northeastern U.S. by exploring several data inputs and outcomes. Using elevation and land cover datasets, we determine where data error is likely, quantify its effect on predictions, and evaluate its influence on prediction confidence. Results show data error is concentrated in low-lying areas with little impact on prediction skill, as the inherent correlation between the datasets can be exploited to reduce data uncertainty using Bayesian inference. This suggests the approach may be extended to regions with limited data availability and/or poor quality. Furthermore, we verify that model sensitivity in these first-order landscape change assessments is well-matched to larger coastal process uncertainties, for which process-based models are important complements to further reduce uncertainty.

1 Introduction

Estimates of global sea-level rise (SLR) predict increases between 0.3 and 1.2 meters by 2100 (Church et al., 2013; Kopp et al., 2014), while Northeastern and Mid-Atlantic U.S. SLR projections are higher than the global average due to a variety of factors including subsidence, static equilibrium effects and changing ocean dynamics (Goddard et al., 2015; Mitrovica et al., 2011; Kopp, et al., 2014; Sella et al., 2009; Slangen et al., 2014; Sweet et al., 2017a,b; Yin & Goddard, 2013; Yin et al., 2009; Zervas et al., 2013). SLR impacts such as high tide flooding, barrier island narrowing, and salt marsh degradation have been increasingly observed along the U.S. East Coast (e.g. Cahoon et al., 2009; Ezer & Atkinson, 2014; Kirwan & Megonigal, 2013; Sweet & Park, 2014). The northeastern U.S. coast (from Maine southward through Virginia) is a diverse landscape, with major shipping ports (eg. New York City, Boston, Norfolk), heavily populated cities (eg. Washington, D.C., New York City, Boston), and extensive natural areas that provide a variety of habitat and ecosystem services. Understanding and assessing how coastal landscapes such as this respond to SLR is central to refining adaptive management strategies (Fishman et al., 2014) and identifying areas that provide buffering or mitigation to support long-term management targets (Pelletier et al., 2015).

Coastal environments are products of a complex interplay of exposure and processes, substrate and sediment supply, tidal ranges, and geomorphology (e.g. Davies, 1964; FitzGerald et al., 2008; Hayes, 1979). As illustrated by Carter (1988), a robust body of literature documents the ecologic transition of these environments from the shoreline over geomorphic features (e.g. dunes and bluffs) landward. In fact, a relatively steady SLR rate over the last few thousand years is central to our modern coastal configuration, including the development of barrier islands and wetlands (e.g., Redfield, 1972; Field & Duane, 1976; Shennan & Horton, 2002), as well as settlement patterns (McGranahan et al., 2007; Liu et al., 2015; Kane et al., 2017). Because coastal land elevation is primarily governed by the substrate and/or underlying geology of the landscape as well as a product of the physical

36 and biogeochemical processes acting on it, it serves as a central parameter in defining the distribution and configuration of
37 ecosystems and their ability to evolve in response to processes driving change (Gesch, 2009; Kempeneers et al., 2009).

38

39 Models are widely available (e.g., Marcy et al. 2011, Strauss et al. 2012) to estimate the potential for SLR-induced inundation
40 across the landscape. These models use present-day elevation as a primary input, which makes them well-suited to identify impacts
41 to developed areas, where hard structures, barriers to migration, and other stabilization measures constrain the landscape to its
42 current elevation and use. However, these models cannot depict landscape variability in environments that respond dynamically
43 to SLR through mechanisms such as vertical accretion due to washover or biomass accumulation. Lentz et al. (2016) addressed
44 this limitation by developing a coastal response model (Figure 2) for the northeastern U.S. that predicts the likelihood of dynamic
45 response to SLR, where *dynamic* is defined as the ability of an environment to either maintain its current state (e.g., a beach remains
46 a beach) or transition to another non-submerged state (e.g., a forest becomes a marsh).

47

48 The confidence of our probabilistic dynamic response outcomes depends on the accuracy of model input parameters, which include
49 continuous land cover and elevation data. Here, we use the nearly 38,000 km² coverage of Lentz et al. (2016) to examine 1) the
50 sensitivity of predictions to differences in the certainty of these input data and 2) model skill to determine where better data are
51 necessary to improve prediction confidence and affect results. We explore the inherent correlation between elevation and coastal
52 land cover distributions in our model by testing the ability of Bayesian inference to capture this relationship such that elevation
53 may be used to predict land cover, and vice versa. We hypothesize that the relationship between these data inputs over such an
54 extensive and diverse expanse reduces uncertainty in each parameter in our framework, and that that potential data error is
55 sufficiently minor that it does not obscure important process thresholds that would in turn affect predicted outcomes. In addition
56 to better understanding model sensitivity to these parameters, our results also clarify how Bayesian inference may be used to
57 supplement poorer data quality and/or uncertainty, particularly in low-lying coastal environments.

58 **2 Data and Methods**

59 **2.1 Previous Work**

60 Lentz et al. (2015) mapped coastal response predictions—the probability of dynamic response or DP—using a Bayesian network
61 (BN) probabilistic modelling approach (Table 1). We define DP as the likelihood of land cover type to retain its existing state or
62 transition to a new non-submerged state under the given SLR projection. By this definition, DP is a binary outcome, in that if the
63 coast does not respond dynamically to SLR, it will inundate, therefore DP equals one minus the probability of inundation. A DP
64 value of 0.5 indicated highest uncertainty in that either dynamic response or inundation had an equally likely probability of
65 occurrence (Lentz et al., 2016).

66

67 The study area was a 38,000 km² region from Maine to Virginia, U.S.A., bounded by the 10-m elevation contour inland to -10 m
68 offshore. The BN (Figure S1) produced two probabilistic outcomes at a 30 x 30 m resolution for future SLR scenarios in the
69 2020s, 2030s, 2050s, and 2080s: 1) adjusted land elevation (AE) relative to the projected sea level, and 2) dynamic response or
70 DP. As described in Lentz et al. (2015), the SLR scenarios were comprised of three components: ocean dynamics (generated from
71 24 Coupled Model Intercomparison Project Phase 5 (CMIP5) models (Taylor et al., 2015), ice melt (as estimated by Bamber and
72 Aspinall, 2013 for the two Antarctic Ice Sheets, and glaciers and ice caps as based on Marzion et al, 2012 and Radic et al., 2013),
73 and global land water storage (as based on Church et al., 2013). Percentiles of these three components were estimated and then

74 aggregated to provide a SLR scenario and corresponding uncertainty. The projected SLR scenario ranges for each decade used in
75 our model are shown in Figure S1 as follows: 2020s (0 to 0.25 m); 2030s (0.25 to 0.5 m); 2050s (0.5 to 0.75 m) and 2080s (0.75
76 to 2 m).

77
78 AE predictions were generated through implementation of a deterministic equation (see Figure S1). First, SLR scenarios were
79 combined with vertical land movement rates due to subsidence and other non-tectonic effects (using rates derived from a
80 combination of GPS CORS stations in Sella et al., 2007; and long-term tide gauge data in Zervas et al., 2013) to make projections
81 relative (local). Projected relative SLR values were then subtracted from elevation data binned in ranges (as shown in Figure S1),
82 which were comprised of a combination of high-resolution elevation data from the National Elevation Dataset (NED, Gesch, 2007)
83 supplemented where necessary with coarser resolution bathymetry from the National Oceanic and Atmospheric Administration
84 National Geophysical Data Center's Coastal Relief Model (National Oceanic and Atmospheric Administration, 2014) to predict
85 adjusted land elevation (AE) ranges relative to the projected sea level. Before model integration, high resolution elevation data
86 were converted to mean high water from the North American Vertical Datum 1988 using VDatum conversion grids (National
87 Ocean Service, 2012).

88
89 Dynamic response probabilities (DP) were estimated by coupling the predicted AE ranges with expert knowledge on the response
90 of generalized land cover types (six categories that respond distinctly to SLR ecologically or morphologically--subaqueous, marsh,
91 beach, rocky, forest, and developed--as described in Lentz et al. (2015) and shown in Table S1). Although the resulting predictions
92 provided a robust accounting of uncertainty from some of the data inputs and knowledge of physical landscape change processes,
93 the relative influence of these uncertainties on the predictions has not been explored explicitly.

94 2.2 Sensitivity and Skill Assessment

95 We assessed the role of potential error in elevation (E) and land cover (LC) datasets on predicted outcomes. Beaches and estuarine
96 wetlands exist near sea-level; likewise, forests require elevations that provide adequate vadose zone thickness. While this
97 correlation between E and LC allows one to be probabilistically predicted from the other, doing so also results in error correlation.
98 Model elevation data came from the National Elevation Dataset (1/9 arc second or 1/3 arc second; U.S. Geological Survey, 2015)
99 and Coastal Relief Model (as described in Lentz et al. 2015). The expected errors in E from these data were included in previous
100 predictions (Lentz et al., 2016), but their effect on predictions was not specifically addressed. Furthermore, the LC values (from
101 McGarrigal et al., 2017) were not treated as uncertain, which was inconsistent with the treatment of all the other relationships in
102 the Lentz et al. (2016) analysis. Better understanding of E and LC error helps to constrain it and identify where better data may
103 improve predictions. Conversely, knowing where data have lower error helps to identify where process uncertainty is highest,
104 which can help prioritize future research efforts.

105
106 We expanded our testing to determine 1) how our LC dataset compares with other LC data and previous error quantification results,
107 2) how E uncertainty is refined by LC information, and 3) where error in LC and E datasets is most likely to affect our predictions.
108 As described in Lentz et al. (2016), inference training (Bayes rule) was applied in the model to capture the correlation between E
109 and LC in the form:

$$110 P(E_i|LC_j) = P(LC_j|E_i) \times P(E_i) / P(LC_j), \quad (1)$$

111 where we evaluate the i^{th} outcome in the first term on the right as the probabilistic relationship conditioned on inputs from the j^{th}
112 spatial location. Using this relationship, LC, entered with total certainty (such that $P(\text{LC}_j)$ is 1.0 if LC_j corresponds to the land
113 cover data at a particular location or $P(\text{LC}_j) = 0.0$ if it does not), updates the prior E, entered with known uncertainty, based on the
114 values of the digital elevation model over the entire modelling domain. Similarly, E data are used to establish conditional
115 probabilities of LC. By assessing potential E and LC error using a BN that implements equation 1 (Figure S1), we can evaluate
116 model skill in reducing error.

117 2.2.1 Land Cover Data Comparison

118 As noted in Lentz et al. (2015), the 2010 land cover data in the model (hereafter DSL, after McGarrigal et al., 2017) combine a
119 variety of sources to capture detailed ecosystems information. To better evaluate land cover data error, we compared land cover
120 data with the 2010 Coastal Change Analysis Program (CCAP) land cover dataset which has a quantified error, (NOAA 2017,
121 <https://www.coast.noaa.gov/dataregistry/search/collection/info/ccapregional>) and were thus used as our “observed” data source.
122 Although the DSL land cover data contain much more detailed ecosystems information than CCAP (19 classes in CCAP vs. 197
123 classes in DSL), our generalization of DSL data into six classes (Table S1) allowed us to similarly generalize CCAP data and
124 compare the two data sets in terms of user’s error (accuracy, or how often the LC type in the DSL data would be the same in the
125 CCAP or “observed” data) and producer’s error (reliability, or how often the LC type in the CCAP or “observed” data would be
126 the same in the DSL data). When generalizing the two datasets for purposes of comparison, we further grouped together beach
127 and rocky categories, as both exposed bedrock and beach/dune categories are included in the CCAP “bare land” category (Table
128 S1). Data grids were compared using ArcGIS software’s Combine tool (ESRI, 2016).

129 2.2.2 Model Skill

130 Our training dataset included E and LC data at ~42,000,000 grid cells throughout the northeast U.S.. We tested our BN (developed
131 with Netica software; Norsys, 2014) and trained on these datasets, to predict E values from LC data, and LC data from E values,
132 by assessing posterior probability distributions in our BN, and evaluating the error rate between predictions and observations. To
133 perform this test, we built a separate two-variable BN to implement equation 1 consisting only of E and LC data (Figure 1). The
134 network was trained on the full elevation and DSL land cover dataset using equation 1, and an error rate was calculated based on
135 the number of times the network predicted a value for a dataset that did not match the observed value at a given location. To test
136 the extension of the inference relationship to situations where E or LC data inputs may be unavailable or limited, the modified BN
137 was used to predict an E value (or LC, as the BNs can be run as both forward and inverse models) as if it were unobserved given
138 only the (uniformly distributed) LC data (or E value) as an input, and the corresponding posterior probabilities were observed.

139 2.2.3 Mismatch Error

140 Some errors were expected from inconsistencies between the LC data and the E data, such as where subaqueous categories (Figure
141 1) co-occurred with elevations above 0 m (referenced to Mean High Water, or MHW in our model), and elevations below 0 m co-
142 occurred with a land cover category other than subaqueous. These mismatches might be due to classification or elevation error,
143 datum changes, or changes over time. To evaluate the impact of these mismatches, we focused on an area contained within the
144 highest resolution and continuous elevation boundary contours (-1 to 10 m from the 1/3 NED), using about half our points
145 (~22,000,000), as we anticipated mismatch errors farther offshore than -1 m would be low (i.e. below 0 m and subaqueous). We
146 classified mismatches by: 1) E data resolution (1/3 and where available, 1/9 arc-second data from the National Elevation Dataset)
147 and 2) LC type to determine whether errors might be explained systematically due to inputs.

148

149 Once identified, we examined the effects of mismatches on the accuracy of predicted outcomes. First, our model was used to
150 identify corresponding DP likelihood among LC types and the low-lying E ranges most commonly mistaken with one another (-1
151 to 0 and 0 to 1 m). Rather than evaluate a specific time step, we made input parameters defining relative SLR uniform (vertical
152 land movement and projected sea level, as in Figure S1) to assess overarching impacts on predictions. Mismatches were also
153 compared geospatially with measured land cover shifts in the 2001 to 2010 CCAP change data (NOAA, 2013) to assess where E
154 and LC data inputs, due to slightly differing dates in their data collection (Lentz et al., 2015) may have captured dynamic state
155 shifts due to process-based changes (e.g. movement of sand bodies around inlets or marsh erosion/inundation; Gomez et al., 2016).

156 **3 Results**

157 **3.1 Land Cover Error**

158 Our LC error assessment found 15% error between CCAP and DSL data; this value is the same as the published 15% error for the
159 CCAP dataset (Table 1 and McCombs et al., 2016). A confusion matrix (Table S2) reveals which LC classes were most commonly
160 mistaken; most frequent were bare land misclassified as subaqueous, and marsh misclassified as non-marsh vegetation.
161 In addition to having the lowest number of pixels of all the land cover classes, user's error and producer's accuracy were lowest
162 for the bare land category (49% and 21% respectively); the least number of correctly classified pixels were in the bare land class
163 when compared with the ground truth (CCAP) class. The bare land class also had the least number of pixels when compared with
164 all other LC categories.

165 **3.2 Model Skill**

166 The two-parameter BN showed that for this implementation, LC was nearly as useful for constraining E as the other way around
167 (Figure 1; Tables S3-S4). Figure 1a shows that when non-uniform E data were used to predict LC, subaqueous environments were
168 the most probable prediction for elevations lower than 0 m (as illustrated by the top four plots on the left). This result reflects, in
169 part, the dominance of subaqueous environments in our data set and therefore strong prior probability that any location below this
170 elevation would be covered by water (Figure S1). Additionally, we developed a modified BN with uniform prior distributions of
171 LC (Figure 1a) and E (Figure 1b) to re-evaluate the inference relationship as if all prior states of the nodes were equally probable,
172 which limits prediction bias from the lower percentage representation of certain land cover categories in the region.

173

174 Generally (for both original and uniform-prior BNs), elevation signatures specific to different land cover types were observed,
175 with subaqueous, marsh, and beach environments appearing at low-lying elevations, and developed and forested areas showing a
176 predominance for higher elevation settings (Figure 1a). When relying on the original prior LC distribution, the network had a
177 corresponding accuracy rate of 69% (Table 1), and found beaches and rocky areas were not more probable than another land cover
178 type. Here, beaches were most commonly confused with subaqueous and marsh land cover types, and rocky areas with subaqueous
179 (Table S3a). Uniformly distributed LC priors yielded slightly different predicted outcomes, wherein the network never found
180 rocky and forested land cover types more probable than another land cover type, most commonly confusing them with subaqueous
181 and developed land cover types respectively (Table S3b). Overall, the accuracy rate in the inference relationship between E and
182 LC was 56% when uniform LC prior distributions were used (Table 1).

183

184 When land cover data were used to predict elevation (Figure 1b), a consistent dependence of the E distribution on the LC data was
185 seen, with E increasing as LC traversed submerged, marsh, beach, rocky, and forested environments. Overall, accuracy and
186 reliability were lowest for the -1 to 0 m and 0 to 1 m ranges with both original and uniform prior distributions of E (Tables S4a
187 and S4b). The difference in prediction using the uniform-prior BN was that the 5-10 m range category was predicted, whereas this
188 elevation was not more probable than another when original priors were used. The accuracy rate in the inference relationship
189 between LC and E was 66% for the original prior distribution and 58% for the uniform priors (Table 1).

190 3.3 Mismatch Error

191 We define a mismatch as a location where the subaqueous LC type co-occurred with elevations above 0 m, or where the remaining
192 LC types co-occurred with elevations below 0 m. The mismatch assessment (Figure 2a) showed that land-water mismatches affect
193 15% of the reduced ($>19,000 \text{ km}^2$) prediction area (Figure 2b) and the most commonly occurring mismatches (Figure 2c) were
194 among dynamic environments (subaqueous, marshes and beaches) at low elevations (-1 to 1 m). More than half of the mismatch
195 data were comprised of LC categories other than subaqueous below 0 m. Of these, nearly all environments were found in the -1
196 to 0 bin, wherein marshes were the dominant environment type (35% of mismatch), followed by beaches (8% of mismatch). The
197 remaining LC types (rocky, forest, developed) comprised $<6\%$ of the observed mismatch area combined. The cumulative
198 probability of the subaqueous category falling in a positive E range (0 to 1 or 1 to 5 m) made up the remainder of the mismatch
199 data (42%), with nearly 78% of these falling within the 0 to 1 m range.

200

201 Mismatches helped to highlight what may be systematic offsets with the E and LC data inputs. The most common mismatches
202 were nearly evenly divided between 1/3 and 1/9 arc-second NED datasets, however mismatch error was more dominantly
203 comprised of elevation data below 0 m sourced to the 1/9 arc-sec NED, and error sourced to the 1/3 arc-second dataset most
204 commonly came from the subaqueous category falling in a positive E range. Mismatch error was also nearly three times as likely
205 to occur in marshes or subaqueous categories as in any other LC category (Figure 2b). In sum, mismatches were most concentrated
206 in low-lying ranges for coastal areas 1) comprised of LC categories (beaches, marshes) most commonly misclassified in the LC
207 comparison (Section 3.1) and 2) where land cover was most inaccurate and unreliable when used in predicting elevation (-1 to 1
208 m, Section 3.2). Using uncertainty terminology as in Mastrandrea et al., 2010, mismatched beaches had a *likely* DP ($P > 0.66$) in
209 both -1 to 0 and 0 to 1 m bins (Figure 2d), whereas the DP for the remaining mismatched land cover categories between -1 to 1 m
210 were *as likely as not* ($0.33 < P < 0.66$; marshes, forests) to *unlikely* ($P > 0.33$; rocky, developed).

211 4 Discussion

212 The high overall agreement between CCAP and DSL data when reclassified (Table S1) indicates DSL data have at most moderate
213 error. Although the elevation data have a stated, calculated error that was integrated directly in our model, a similar error estimate
214 was not available for the land cover (DSL) data (although our probabilistic framework allows this to be incorporated if available).
215 Comparing the DSL land cover dataset to a dataset with a known error value (CCAP), revealed an identical error rate (15%) to that
216 determined for CCAP alone (McCombs et al., 2016). Although we cannot confirm that this error resides solely with the CCAP
217 data, the updated and more detailed information in the DSL data, as well as the similarity in error rate with the published CCAP
218 error, suggests that entering the DSL data as if they are known with certainty is an appropriate assumption for most of our LC
219 categories.

220

221 The land cover comparison also showed that bare land and marsh categories are those most commonly classified as another
222 category (subaqueous and non-marsh vegetation respectively). The greatest error in the comparison--the bare land category—is
223 in part explained by the substantial under-representation of beaches in both datasets when compared with other LC types. Due to
224 this under-representation, beaches are never the most probable land cover type predicted from E when original prior distributions
225 are applied (Table 3a). Our uniform prior test demonstrates that in spite of this regional bias, there is also ambiguity in the E-LC
226 relationship in with regards to beaches and marshes in our model; when either marshes are beaches are predicted from E with a
227 uniform prior, they match the observed LC (user's accuracy) 47-49% of the time respectively (Table S3b). However, beaches are
228 more confidently predicted in the -1 to 0 m range than other land cover types (Figure 1b), suggesting a propensity of beaches in
229 our model training data are shallowly submerged. Incorporating first-return lidar instead of bare earth data in our model could be
230 used to further distinguish the six LC types from one another via vegetation differences (e.g. Lee and Shan, 2003; Im et al., 2008;
231 Reif et al., 2011) and better distinguish intertidal areas, which may allow refinement of marsh, beach, and forest classifications
232 (e.g. Kepeneers et al., 2009; Sturdivant et al., 2017).

233
234 Testing our two-node BN revealed that Bayesian inference can be used to fill data gaps or enhance data quality. Applying both
235 non-uniform and uniform priors (the latter to remove the regional land cover biases specific to the northeastern U.S.) showed that
236 land cover-specific elevation signatures are present. Notable distinctions were between elevation end members (very high or very
237 low relief; subaqueous, forests, developed) and mid-range (moderate relief; marshes, beaches, rocky) areas. Assessing model skill
238 in the E and LC relationship revealed an accuracy of 56% (uniform priors) to 69% (non-uniform priors), showing that including
239 the regional LC bias helped to improve predictions (Table 1), and that the most commonly missed LC-E predictions occurred in
240 elevations closest to mean sea level (-1 to 1 m).

241
242 In addition to missed predictions, our testing revealed that some E ranges and LC categories were never the most probable outcome.
243 This was true for several land cover types (specifically beaches and rocky under original E priors; rocky and forest under uniform
244 priors (Tables S3) and one elevation range (5-10 m elevations under original LC priors, Table S4b). For the original priors, we
245 attribute this to the under-representation of certain classes (regional bias) in our training data, wherein beaches, rocky, and 5-10 m
246 elevation ranges were infrequent when compared to other classes/bins. In the case of uniform priors, our BN is detecting the
247 slightly stronger relationship of some land cover types in certain elevation ranges (e.g. developed in the 1 to 5 m range), thereby
248 making other E-LC relationships never more probable than these. Although bin reassignments that span smaller elevation ranges
249 could help resolve more specific land cover signatures in our model, particularly for low-lying beaches and marshes, this would
250 likely occur at the cost of increased prediction uncertainty as outcomes would span a larger number of bins.

251
252 Our mismatch analysis revealed LC and E mismatches are uncommon and found at low elevations (-1 to 1 m) in dynamic
253 environments (beaches, marshes, and subaqueous categories). Mismatches were most infrequent among typically higher elevation
254 environments (forests, developed, and rocky). We suggested that low elevation mismatches resulted from physical changes, such
255 as tidal inlets causing submerged sandbars to become subaerial beach, or forests becoming marshes. However, comparison with
256 CCAP changes from 2001 to 2010, revealed a very small (3%) correspondence with identified areas of mismatch. Results instead
257 may suggest high-resolution (1/9 NED) E data captures a systematic offset in part due to MHW submergence from datum
258 conversion (Lentz et al., 2015), particularly for marshes and beaches (Fig 3b). In addition to elevation data that accounts for
259 vegetation, as suggested earlier, seamless and continuous topographic and bathymetric data (Danielson et al., 2016) would
260 constrain resolution error and better resolve distinctions between subaerial and subaqueous environments.

261

262 Ultimately, the contributions of data error are unlikely to change the DP uncertainty categories (Fig. 2d). In the case of LC error,
263 the most commonly confused LC categories were subaqueous with beach categories, and marshes with forests. In either case,
264 when coupled with E data, beaches and subaqueous categories between -1 and 1 m generally have a *likely* DP and marshes and
265 forests to have an *as likely as not* DP (Figure 2d), with the latter emphasizing the dominance of process uncertainty as accounted
266 for in our original model via expert elicitation (as described in Lentz et al., 2015) over data error in affecting DP outcomes.
267 Furthermore, the response of developed and some beach areas to SLR is also particularly uncertain in our model due to unknowns
268 regarding human behaviour (Wong et al., 2014). Socioeconomic factors (McNamara et al., 2011, Hinkel et al., 2013) may
269 determine where buildings and critical infrastructure are adapted to a dynamically changing landscape, coastal engineering projects
270 are employed or upgraded (Gedan et al., 2011; Arkema et al., 2013), and alternatives such as inland migration (Hauer et al., 2016;
271 2017) or managed retreat occur. Our probabilistic modelling framework allows us to update likelihood predictions as more
272 information about the SLR response of the coastal landscape, and people living on it, becomes available.

273 **5 Conclusions**

274 Our results show that a) land cover error between two data sources is consistent with published error for one source (15%), b)
275 inference training further reduces error, and c) mismatch error is low with respect to the prediction area. To better resolve elevation
276 and land cover distinctions in low-lying environments, elevation that accounts for vegetation distinctions, and/or seamless datasets
277 including both topography and bathymetry may be useful. However, the ability to capture the relationship between elevation and
278 land cover via Bayesian inference in such a sizeable region demonstrates that it is possible to extend this application where data
279 restrictions or gaps might otherwise limit expansion.

280

281 Furthermore, data input error has minimal effect on our predicted outcomes, particularly when uncertainty terminology is applied
282 (Figure 2d). These outcomes therefore support first-order decision-making surrounding the inundation potential of specific
283 environments, providing an essential risk assessment tool (NRC, 2009). We find uncertainty in the response of different land cover
284 types to varying SLR scenarios in our coastal response model is composed dominantly of uncertainty in physical and ecological
285 processes, as opposed to data error, particularly for developed areas and low elevation marshes (Lentz et al., 2016). To further
286 refine assessments of future coastal response in areas of concern, data or deterministic models that account for site-specific SLR
287 response rates and process knowledge will be well-paired with this approach.

288

289 **Data Availability**

290 Coastal response outcomes: Lentz, E.E., Stippa, S.R., Thieler, E.R., Plant, N.G., Gesch, D.B., and Horton, R.M. 2015, Coastal
291 landscape response to sea-level rise assessment for the northeastern United States (ver. 2.0., December 2015): U.S. Geological
292 Survey data release, <http://dx.doi.org/10.5066/F73J3B0B>.

293 **Supplement link (tbd)**

294 **Author Contributions**

295 EEL and NGP designed the study; EEL the conducted analysis; and EEL, ERT, and NGP drafted the initial version of the
296 manuscript. All authors discussed results and contributed to later versions of the manuscript.

297 **Acknowledgments and Disclaimer**

298 This research was funded by the U.S. Geological Survey Coastal and Marine Geology Program. Data used in this analysis can be
299 downloaded at: https://woodshole.er.usgs.gov/project-pages/coastal_response/data.html. We thank Neil Ganju for early reviews
300 and discussion of this manuscript. Any use of trade, firm, or product names is for descriptive purposes only and does not imply
301 endorsement by the US Government. The authors declare no that they have no conflicting interest.

303 **References**

- 304 Arkema, K.K., Guannel, G., Verutes, G., Wood, S.A., Guerry, A., Ruckelshaus, M., Karejva, M., Lacayo, M., and Silver,
305 J.M.: Coastal habitats shield people and property from sea-level rise and storms. *Nat. Clim. Change*, 3, 913-918.
306 <https://doi.org/10.1038/nclimate1944>, 2013.
- 307 Cahoon, D.R., Reed, D.J., Kolker, A.S., Brinson, M.M., Stevenson, J.C., Riggs, S., Christian, R., Reyes, E., Voss, C., &
308 Kunz, D.: Coastal wetland sustainability. In J.G. Titus, K.E. Anderson, D.R. Cahoon, D.B. Gesch, S.K. Gill, B.T.
309 Gutierrez, B.T., E.R. Thieler, & S.J. Williams, *Coastal sensitivity to sea-level rise— A focus on the mid-Atlantic region*:
310 Washington, D.C., U.S. Environmental Protection Agency, pp. 57– 72, 2009.
- 311 Carter, R.: *Coastal environments: an introduction to the physical, ecological, and cultural systems of coastlines*. Academic:
312 San Diego, CA, 1988.
- 313 Church, J.A., Clark, P.U., Cazenave, A., Gregory, J.M., Jevrejeva, S., Levermann, A., Merrifield, M.A., Milne, G.A., Nerem,
314 R.S., Nunn, P.D., Payne, A.J., Pfeffer, W.T., Stammer, D., & Unnikrishnan, A.S.: Sea level change. In T.F. Stocker, D.
315 Qin, G-K Plattner, M. Tignor, S.K. Allen, J. Boschung, A. Nauels, Y. Xia, V. Bex, V., & P.M. Midgley, (Eds.),
316 *Climate Change 2013: The Physical Science Basis* (Contribution of Working Group I to the Fifth Assessment Report of
317 the Intergovernmental Panel on Climate Change). Cambridge, United Kingdom and New York, NY, USA: Cambridge
318 University Press, 2013.
- 319 Danielson, J.J., Poppenga, S.K., Brock, J.C., Evans, G.A., Tyler, D.J., Gesch, D.B., Thatcher, C.A., and Barras, J.A.:
320 Topobathymetric elevation model development using a new methodology-Coastal National Elevation Database. *J.*
321 *Coastal Res.*, SI(76), 75-89. <http://dx.doi.org/10.2112/SI76-008>, 2016.
- 322 Davies, J.L.: A morphogenic approach to world shorelines. *Z. Geomorphol.*, 8, 27-42, 1964.
- 323 ESRI: ArcGIS Desktop: Release 10. Redlands, CA: Environmental Systems Research Institute, 2016.
- 324 Ezer, T. and Atkinson, L. P.: Accelerated flooding along the U.S. East Coast: On the impact of sea-level rise, tides,
325 storms, the Gulf Stream, and the North Atlantic Oscillations. *Earth's Future*, 2, 362–382, 2014.
- 326 Fischman, R.L., Meretsky, V.J., Babko, A., Kennedy, M., Liu, L., Robinson, M., and Wambugu, S.: Planning for
327 adaptation to climate change: Lessons from the US National Wildlife Refuge System. *BioScience*, 64(11), 993-1005,
328 2014.
- 329 FitzGerald, D.M., Fenster, M.S., Argow, B.A., and Buynevich, I.V.: Coastal impacts due to sea-level rise. *Annu.*
330 *Rev. of Earth Planet. Sci.*, 36(1), 601-647, 2008.
- 331 Field, ME., and Duane, D.B.: Post-Pleistocene history of the United States inner continental shelf: Significance to
332 origin of barrier islands. *Geol. Soc. Am. Bull.*, 87(5): 691–702, 1976.
- 333 Gedan, K.B., Kirwan, M.L., Wolanski, E., Barbier, E.B. & Silliman, B.R.: The present and future role of
334 coastal wetland vegetation in protecting shorelines: Answering recent challenges to the paradigm. *Clim. Change*,
335 7-29, 2011.
- 336 Gesch, D.B., The national elevation dataset, chap. 4 of Maune, D.F., ed., *Digital elevation model technologies*
337 *and applications—The DEM users manual (2d ed.)* (pp.99-118). Bethesda, Md.: American Society for Photogrammetry
338 and Remote Sensing.
- 339 Gesch, D.B.: Analysis of lidar elevation data for improved identification and delineation of lands vulnerable to

340 sea-level rise. *J. Coastal Res.*, SI(53), 49-58, 2009.

341 Gomez, C., White, J.C., and Wulder, M.A.: Optical remotely sensed time series data for land cover classification: A
342 review. *ISPRS Journal of Photogrammetry and Remote Sensing*, 116, 55-72, 2016.

343 Hayes, M.O.: Barrier island morphology as a function of tidal and wave regime, In S.P Leatherman (Ed.), *Barrier*
344 *Islands from the Gulf of St. Lawrence to the Gulf of Mexico* (pp. 1-27). New York, NY: Academic, 1979.

345 Goddard, P.B., Yin, J., Griffies, S.M., and Zhang, S.: An extreme event of sea-level rise along the Northeast coast of
346 North America in 2009-2010. *Nat. Commun.*, 6, 6346, 2015.

347 Hauer, M.E., Evans, J.M., and Mishra, D.R.: Millions projected to be at risk from sea-level rise in the continental
348 United States. *Nat. Clim. Change*, 6, 691-695, 2016.

349 Hauer, M.E.: Migration induced by sea-level rise could reshape the US population landscape. *Nat. Clim.*
350 *Change*, 7, 321-325, 2017.

351 Hinkel, J., Lincke, D., Vafeidis, A.T., Perrette, M., Nicholls, R.J., Tol, R.S. J., Marzeion, B., Fettweis, X., Ionescu, C., and
352 Levermann, A.: Coastal flood damage and adaptation costs under 21st century sea-level rise. *Proceedings of the*
353 *National Academy of Sciences*, 111(9), 3292-3297, 2014.

354 Im, J., Jensen, J.R., and Hodgson, M.E.: Object-based land cover classification using high-posting-density lidar data.
355 *GIScience and Remote Sensing*, 45(2), 209-228, 2008.

356 Kane, H., Fletcher, C., Cochrane, E., Mitrovica, J., Habel, S., and Barbee, M.: Coastal plain stratigraphy records
357 tectonic, environmental, and human habitability changes related to sea-level drawdown, 'Upolu, Samoa. *Quat. Res.*,
358 87(2), 246-257, 2017.

359 Kempeneers, P. Deronde, B., Provoost, S. and Houthuys, R.: Synergy of airborne digital camera and lidar data to
360 map coastal dune vegetation. *J. Coastal Res.*, SI 53, 73-82, 2009.

361 Kirwan, M.L. and Megonigal, J.P.: Tidal wetland stability in the face of human impacts and sea-level rise. *Nature*,
362 504, 53-60, 2013.

363 Kopp, R.E.: Does the mid-Atlantic United States sea level acceleration hot spot reflect ocean dynamic variability?
364 *Geophys. Res. Lett.*, 40(15), 3981-3985, 2013.

365 Kopp, R. E., Horton, R. M., Little, C. M., Mitrovica, J. X., Oppenheimer, M., Rasmussen, D. J., Strauss, B. H. and Tebaldi,
366 C.: Probabilistic 21st and 22nd century sea-level projections at a global network of tide-gauge sites. *Earth's*
367 *Future*, 2, 383–406, 2014.

368 Lee, D.S. & Shan, J.: Class-guided building extraction from Ikonos imagery. *Photogrammetric Engineering &*
369 *Remote Sensing*, 2, 143-150, 2013.

370 Lentz, E.E., Thieler, E.R., Plant, N.P, Stippa, S.R., Horton, R., and Gesch, D.B.: Evaluation of dynamic coastal
371 response to sea-level rise modifies inundation likelihood. *Nat. Clim. Change*, 6, 696-700, 2016.

372 Lentz, E.E., Stippa, S.R., Thieler, E.R., Plant, N.G., Gesch, D.B., and Horton, R.M.: *Evaluating coastal landscape*
373 *response to sea-level rise in the northeastern United States—Approach and methods* (OFR 2014-1252). U.S.
374 Geological Survey, 2015.

375 Liu, J., Wen, J., Huang, Y., Shi, M., Meng, Q., Ding, J., Xu, H.: Human settlement and regional development in the
376 context of climate change: A spatial analysis of low elevation coastal zones in China. *Mitigation and Adaptation*
377 *Strategies for Global Change*, 20(4), 527-546, 2015.

378 Marcy, D, Brooks, W., Draganov, K., Hadley, B., Haynes, C., Herold, N., McCombs, J., Pendleton, M., Ryan, S., Schmid,
379 K., Sutherland, M., & Waters, K.: New mapping tool and techniques for visualizing sea-level rise and
380 coastal flooding impacts, in: Wallendorf, L., Jones, C., Ewing, L., and Battalio, B. (Eds.), *Solutions to Coastal*
381 *Disasters 2011*, American Society of Civil Engineers, Reston, VA, 474–490, 2011.

382 Marzion, B., Jarosch, A.H., and Hofer, M.: Past and future sea-level change from the surface mass balance of glaciers: *The*
383 *Cryosphere*, 6(6), 1295–1322, 2012.

384 Mastrandrea, M.D., Field, C.B., Stocker, T.F., Edenhofer, O., Ebi, K.L., Frame, D.J., Held, H., Kriegler, E., Mach, K.J.,
385 Matschoss, P.R., Plattner, G.-K., Yohe, G.W., and Zwiers, F.W.: *Guidance Note for Lead Authors of the IPCC Fifth*
386 *Assessment Report on Consistent Treatment of Uncertainties*. Intergovernmental Panel on Climate Change (IPCC),
387 2010.

388 McCombs, J.W., Herold, N.D., Burkhalter, S.G, and Robinson, C.J.: Accuracy assessment of NOAA Coastal Change
389 Analysis Program 2006-2010 Land Cover and Land Cover Change Data. *Photogrammetric Engineering and*
390 *Remote Sensing*, 82(9), 711-718, 2016.

391 McGarigal K, Compton BW, Plunkett EB, Deluca WV, & Grand J.: *Designing sustainable landscapes: DSLland and*
392 *Subsysland*. Report to the North Atlantic Conservation Cooperative, US Fish and Wildlife Service, Northeast
393 Region: (http://jamba.provost.ads.umass.edu/web/LCC/DSL_documentation_DSLland.pdf), 2017.

394 McGranahan, G., Balik, D., and Anderson, B.: The rising tide: assessing the risks of climate change and human
395 settlements in low elevation coastal zones. *Environment and Urbanization*, 19, 17-37, 2007.

396 McNamara, D.E., Murray, A.B. and Smith, M.D.: Coastal sustainability depends on how economic and coastline
397 responses to climate change affect each other. *Geophys. Res. Lett.*, 38, L07401: 1-5, 2011.

398 Mitrovica, J.X., Gomez, N., Morrow, E., Hay, C., Latychev, K., and Tamisiea, M.E.: On the robustness of
399 predictions of sea level fingerprints. *Geophys. J. Int.*, 187, 729-742, 2011.

400 National Research Council: Science and Decisions: Advancing Risk Assessment. The National
 401 Academies Press, Washington DC: 422 p., 2009.

402 National Oceanic and Atmospheric Administration National Geophysical Data Center, U.S. coastal relief model: National
 403 Oceanic and Atmospheric Administration National Geophysical Data Center Web page, last access 9 June 2014 at
 404 <http://www.ngdc.noaa.gov/mgg/coastal/crm.html>.

405 National Oceanic and Atmospheric Administration, Office for Coastal Management. 2010 Coastal Change Analysis Program
 406 (C-CAP) Regional Land Cover. www.coast.noaa.gov/ccapftp, last access: 5 June 2017.

407 NOAA's Coastal Change Analysis Program (C-CAP) 2001 to 2010 Regional Land Cover Change Data - Coastal United
 408 States: Department of Commerce (DOC), National Oceanic and Atmospheric Administration (NOAA), National Ocean
 409 Service (NOS), Office for Coastal Management (OCM),
 410 <https://coast.noaa.gov/dataregistry/search/dataset/info/ccapregional>, 2013, last access: 5 June 2017.

411 Norsys, 1992-2013. Netica 5.12.

412 Pelletier, J.D., Murray, A.B., Pierce, J.L., Bierman, P.R., Breshears, D.D., Crosby, B.T., Ellis, M., Foufoula-Georgiou,
 413 E., Himsath, A.M., Houser, C., Lancaster, N., Marani, M., Merritts, D.J., Moore, L.J., Pederson, J.L., Poulous, M.J.,
 414 Rittenour, T.M., Rowland, J.C., Ruggiero, P., Ward, D.J., Wickert, A.D., Yager, E.M.: Forecasting the response of
 415 Earth's surface to future climatic and land use changes: A review of methods and research needs. *Earth's Future*, 3,
 416 220-251, 2015.

417 Radić, V., Bliss, A., Beedlow, C.D., Hock, R., Miles, E., and Cogley, J.G.: Regional and global projections of twenty-first
 418 century glacier mass changes in response to climate scenarios from global climate models: *Climate Dynam.* 42 (1–2),
 419 37–58, 2013.

420 Redfield, A.C.: Development of a New England salt marsh. *Ecol. Monogr.*, 42, 201–237, 1972.

421 Reif, M.K., Macon, C.L., Wozencraft, J.M., Post-Katrina land cover, elevation, and volume change assessment along
 422 the south shore of Lake Pontchartrain, Louisiana, U.S.A. *J. Coastal Res.*, SI 62, 30-39, 2011.

423 Sella, G.F., Stein, Seth, Dixon, T.H., Craymer, Michael, James, T.S., Mazzotti, Stephane, and Dokka, R.K.:
 424 Observation of glacial isostatic adjustment in “stable” North America with GPS. *Geophys. Res. Lett.*, 34(2), L02306, 6
 425 p., 2007.

426 Shennan, I., and Horton, B.: Holocene land- and sea-level changes in Great Britain. *Journal of Quaternary Science*,
 427 17(5-6), 2002.

428 Slangen, A.B.A., Church, J.A., Zhang, X., and Monselesan, D.: Detection and attribution of global mean
 429 thermosteric sea level change. *Geophys. Res. Lett.*, 41: 5951-5959, 2014.

430 Strauss, B.H., Ziemiński, R., Weiss, J.L., and Overpeck, J.T.: Tidally adjusted estimates of topographic vulnerability
 431 to sea level rise and flooding for the contiguous U.S. *Environ. Res. Lett.*, 7, 014033, 2012.

432 Sturdivant E., Lentz E.E., Thieler, E. R., Farris, A., Weber, K., Remsen, D., Miner, S., & Henderson R.: UAS-SfM
 433 for coastal research: Geomorphic feature extraction and land cover classification from high-resolution elevation and
 434 optical imagery. *Remote Sens.*, 9 (10), 1020, 2017.

435 Sweet, W. V. and Park, J.: From the extreme to the mean: Acceleration and tipping points of coastal inundation from
 436 sea level rise. *Earth's Future*, 2, 579–600, 2014.

437 Sweet, W. V., Kopp, R.E., Weaver, C.P., Obeysekera, J., Horton, R.M., Thieler, E.R., and Zervas, C.: *Global and*
 438 *Regional Sea Level Rise Scenarios for the United States*. NOAA Technical Report NOS CO-OPS 083. NOAA/NOS
 439 Center for Operational Oceanographic Products and Services, 75 p., 2017a.

440 Sweet, W.V., Horton, R., Kopp, R.E., LeGrande, A.N., and Romanou, A.: Sea Level Rise. In D.J. Wuebbles, D.W.
 441 Fahey, K.A. Hibbard, D.J. Dokken, B.C Stewart, & T.K. Maycock (Eds.), *Climate Science Special Report: Fourth*
 442 *National Climate Assessment, Volume 1* (pp. 333-363). U.S. Global Change Research Program: Washington DC:
 443 2017b.

444 Taylor, K.E., Stouffer, R.J., and Meehl, G.A.: An overview of CMIP5 and the experiment design: *B. Am. Math. Soc.*, 93(4), p.
 445 485–498, 2012.

446 U.S. Geological Survey: NED spatial metadata: <http://ned.usgs.gov/downloads.html>, last accessed: 2 January 2015.

447 Wong, P.P., Losada, I.J., Gattuso, J.-P., Hinkel, J., Khattabi, A., McInnes, K.L., Saito, Y., and Sallenger, A.: Coastal
 448 systems and low-lying areas. In C.B. Field, V.R. Barros, D.J. Dokken, K.J. Mach, M.D. Mastrandrea, T.E. Bilir, M.
 449 Chatterjee, K.L. Ebi, Y.O. Estrada, R.C. Genova, B. Girma, E.S. Kissel, A.N. Levy, S. MacCracken, P.R. Mastrandrea,
 450 and L.L. White (Eds.). *Climate Change 2014: Impacts, Adaptation, and Vulnerability. Part A: Global and Sectoral*
 451 *Aspects* (pp. 361-409). Contribution of Working Group II to the Fifth Assessment Report of the Intergovernmental
 452 Panel on Climate Change. Cambridge University Press: Cambridge, United Kingdom and New York, NY, USA: 2014.

453 Yin, J., and Goddard, P.B.: Oceanic control of sea level rise patterns along the East Coast of the United States.
 454 *Geophys. Res. Lett.*, 40, 5514–5520, 2013.

455 Yin, J., Schlesinger, M.E., and Stouffer, R.J.: Model projections of rapid sea-level rise on the northeast coast of the
 456 United States. *Nat. Geosci.*, 2: 262-266, 2009.

457 Zervas, C., Gill, S., and Sweet, W.: *Estimating Vertical Land Motion from Long-Term Tide Gauge Records*. NOAA
 458 Technical Report NOS CO-OPS 065, 30 p., 2013.

460

461 **Table 1.** Summary table of accuracy rates for all confusion matrices of land cover and elevation comparisons. Accuracy rates are
 462 calculated by summing where predictions matched observations (the diagonal bolded terms in Tables S2-S4) and dividing by the
 463 total number of outcomes. Confusion matrices are available in supplemental materials (Tables S2-S4).

464

465

466

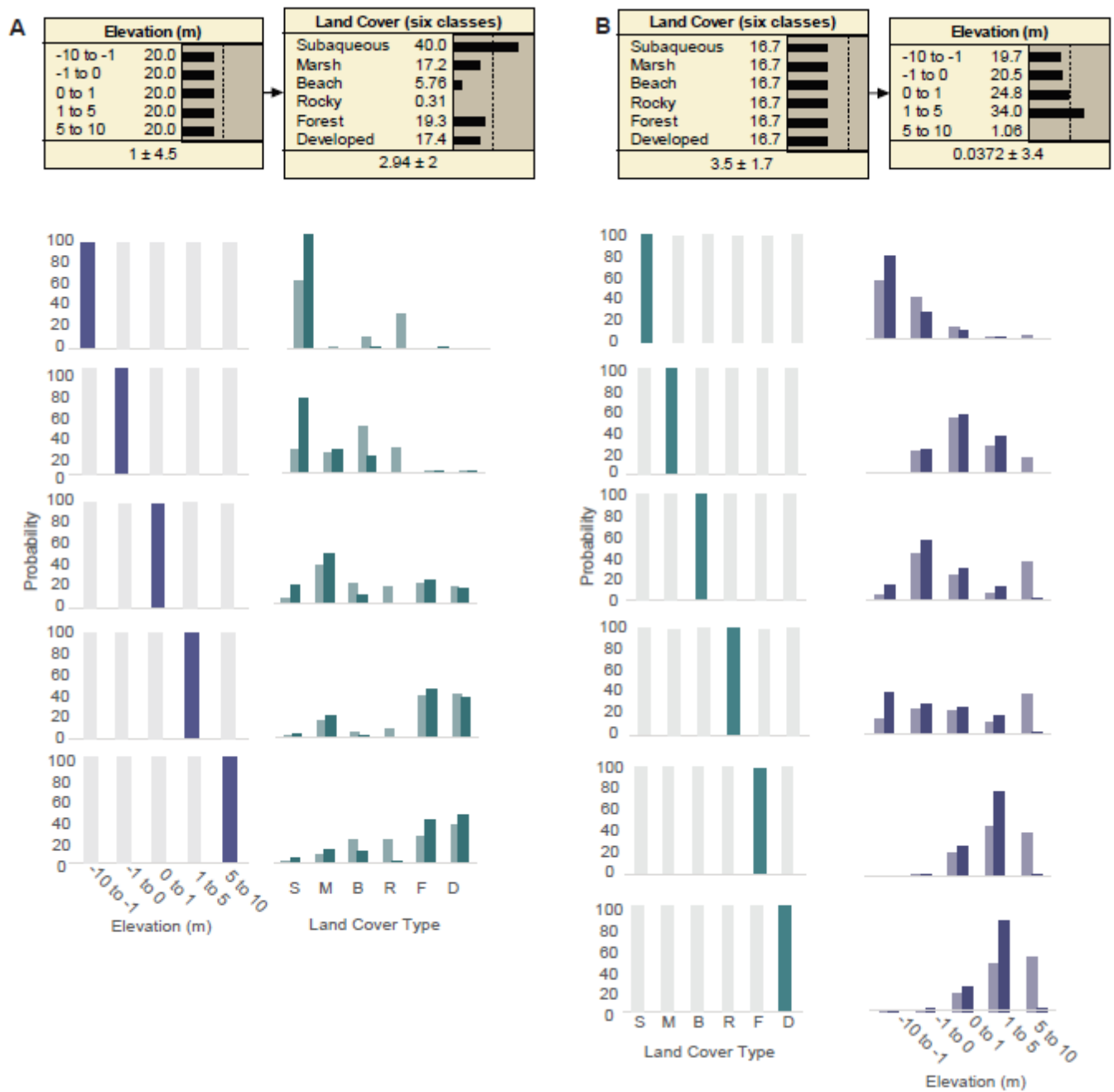
467

468

469

470

Confusion Matrix	Accuracy Rate
C-CAP vs. DSL Land Cover comparison	85%
Predicted vs. Observed Land Cover <i>Elevation inputs; original distributions</i>	77%
Predicted vs. Observed Land Cover <i>Elevation inputs; uniform distributions</i>	65.5%
Predicted vs. Observed Elevation <i>Land cover inputs; original distributions</i>	66%
Predicted vs. Observed Elevation <i>Land cover inputs; uniform distributions</i>	59%



471
 472 **Figure 1.** Updated probability distributions after training between elevation and land cover datasets with non-uniform (dark) and
 473 uniform (light) priors (the latter to limit regional LC bias), a) showing land cover distributions under selected elevation ranges and
 474 b) showing elevation distributions under selected land cover types. Land cover categories (Table S1) abbreviated as follows: S =
 475 subaqueous; M = marsh; B = beach; R = rocky; F = forest; and D = developed.

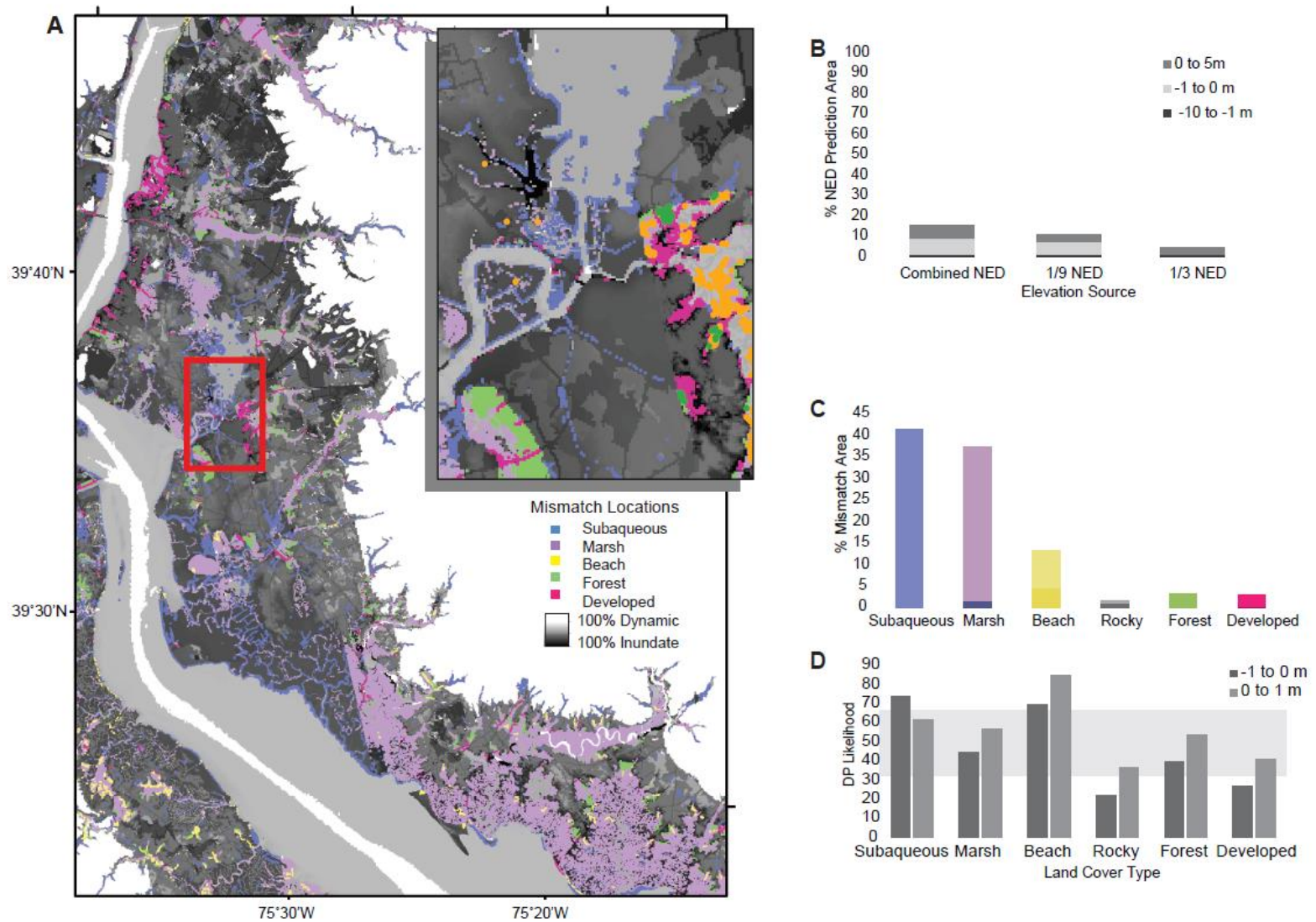


Figure 2. Results of mismatch analysis a) in selected area with inset of enlarged view; b) shown as percentage of the prediction area within the 1/3 National Elevation Dataset (NED) contour boundary and by elevation source type; c) by land cover type as a percentage of the total mismatch area, where lighter hues show the percent of predictions in the -1 to 0 m range (with the exception of subaqueous, which shows a 0 to 1 m range), and darker hues show the percent of predictions in the -10 to 1 m range; and d) the

corresponding probability of dynamic response (DP) likelihood for each land cover type in the elevation ranges most commonly mistaken (light gray box shows the as likely as not likelihood range ($0.33 > P > 0.66$) following Mastrandrea et al., 2010).